NASA TECHNICAL MEMORANDUM
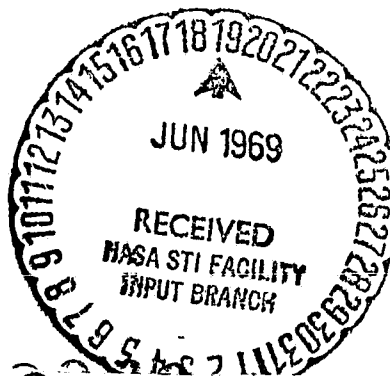
Report No. 53834

STABILIZATION AND CONTROL OF THE APOLLO TELESCOPE MOUNT

By W. B. Chubb
Astrionics Laboratory

May 6, 1969

JUN 1969

RECEIVED
NASA STI FACILITY
INPUT BRANCH

N70-41089

FACILITY FORM 602

(ACCESSION NUMBER)   (THRU)

30

(PAGES)   (CODE)

TmX-53834

(NASA CR OR TMX OR AD NUMBER)   21

(CATEGORY)

NASA

George C. Marshall Space Flight Center

Marshall Space Flight Center, Alabama

PRECEDING PAGE BLANK NOT FILMED.

TABLE OF CONTENTS

LIST OF ILLUSTRATIONS

LIST OF TABLES

STABILIZATION AND CONTROL OF THE APOLLO TELESCOPE MOUNT

INTRODUCTION

The Apollo Telescope Mount (ATM) is a manned solar observatory. The broad objective of ATM experiments is to increase our knowledge of the solar environment by observing it from a station above the major portion of the earth's atmosphere. It is being developed for launch during the first quarter of 1972.

The ATM with its associated cluster (Figure 1) will be placed in 334 km (180 Nm) circular orbit at an orbital inclination relative to the earth's equatorial plane of 35 degrees. A manned flight duration of 56 days is planned. This is to be followed by an unmanned storage mode in which a limited amount of experimental data will continue to be gathered.
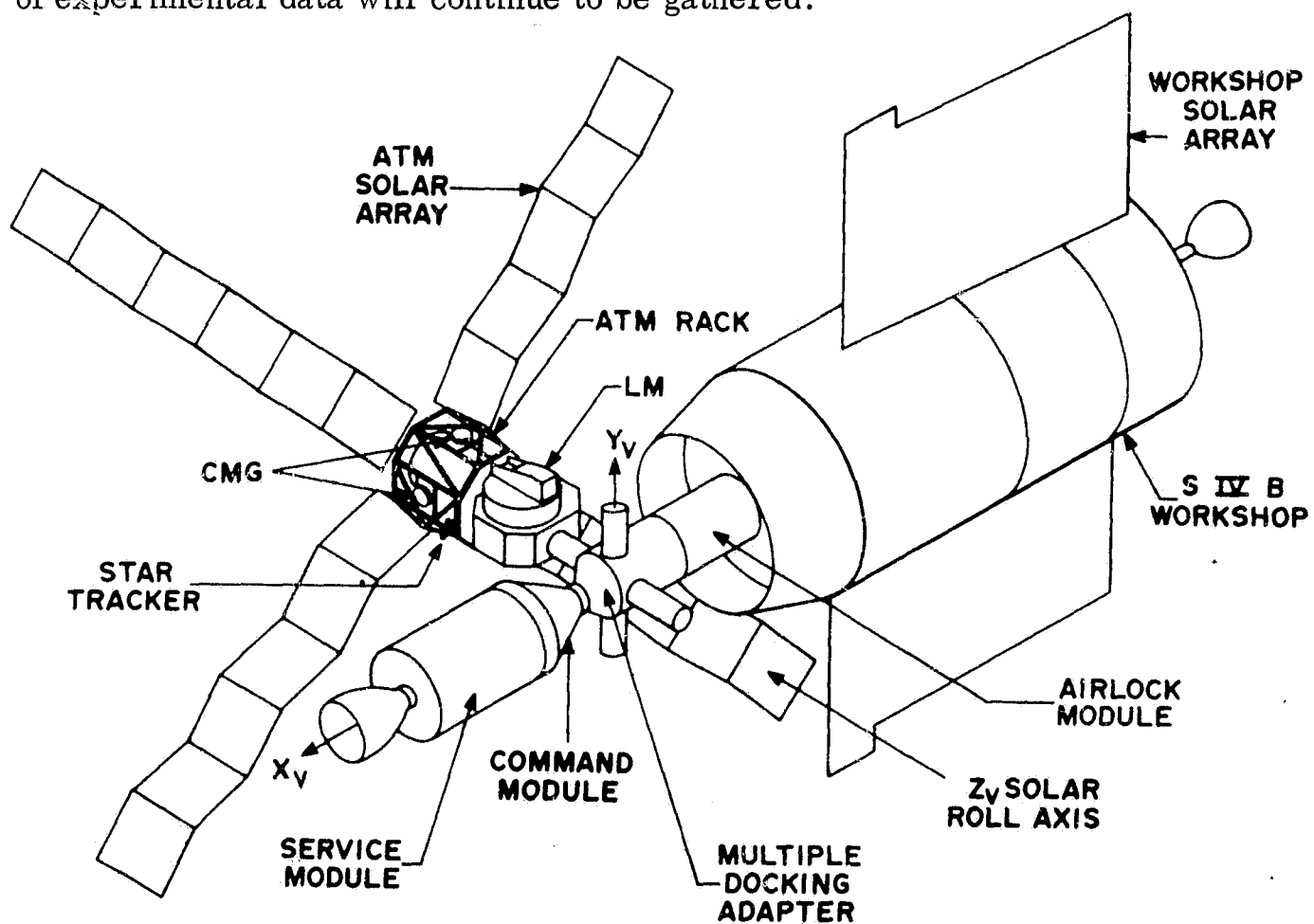

FIGURE 1. APOLLO APPLICATIONS PROGRAM FLIGHTS 3 AND 4

The major objectives of the ATM are as follows:

1. To obtain specific data on the characteristics of the sun through observation of various portions of its electromagnetic spectrum.

2. To obtain engineering data for aid in the design and establishment of future manned solar and stellar observatories.

To meet the scientific objectives of the ATM mission, it was necessary to develop an ATM pointing and control subsystem (PCS) which would meet the high accuracy pointing requirements of the ATM experiments under both external and internal disturbances such as gravity gradient, aerodynamic, and on-board astronaut motion. It was also necessary to minimize the expulsion of mass from the vehicle when taking scientific data to avoid contamination of the sensitive elements of the various ATM experiments. A third consideration was that of keeping the weight of the system to a minimum.

The developed PCS was divided into two major pointing and control subsystems, one to provide pointing and control of the cluster and the other to provide fine pointing and control of the experiment spar. In compliance with mission objectives, a momentum exchange device was chosen as the control torque source for cluster control. The momentum exchange device selected was the control moment gyro (CMG), and the subsystem using CMG's as actuators was the "CMG control subsystem." The fine pointing and control requirements of the spar resulted in the development of a control system using flex-pivot gimbal bearings* for control about two axes and an open loop roll crank-around device to meet positioning requirements about the third axis. Dynamic control about the third axis is supplied by the CMG control subsystem. The control system associated with fine pointing and control of the spar is known as the experiment pointing and control subsystem (EPC).

SYSTEM REQUIREMENTS

The ATM/PCS is required to point an experiment spar to any spot on or near the solar disc and, in the face of disturbance torques (Table I)

---

* A flex-pivot gimbal bearing is made of a pair of flat cross-leaf springs, is welded to and supported by rotating sleeves, has no backlash, and provides limited angular travel.

encountered by the manned space station in its 334-km circular orbit, to maintain its required pointing accuracy and stability as illustrated in Table II* .

TABLE I. MAJOR DISTURBANCE TORQUES

Disturbance Torque	Peak Torque (Nm)	Frequency
Gravity gradient	8	Twice orbital period
Aerodynamic	2	Orbital period
Magnetic	0.16*	Orbital period
Man motion	720	Predominantly 0.1 to 1 Hz
Venting and gas leakage	Not specified	Variable
* Maximum average torque per orbit		

TABLE II. POINTING ACCURACY AND STABILITY

System	Pointing	Stability (For 15 min)
CMG roll	±10 arc min	±7.5 arc min
CMG pitch and yaw	±4 arc min	±9 arc min
EPC roll	±10 arc min	---
EPC pitch and yaw	±2.5 arc sec	±2.5 arc sec

---

* For the PCS design requirements, roll is defined as the angular rotation about the line of sight from the experiment package to the center of the sun, and pitch and yaw are the small angular deviations of the experiment package with respect to this line of sight.

These pointing requirements are illustrated in Figure 2 which portrays the experiment package reference axis offset from the line of sight to the center of the sun by the maximum offset angle ϕ_o of 20 arc min (solar radius is 16 arc min). At this offset angle and because of the ± 10 arc min uncertainty of the roll angle ϕ_r, the commanded point in the plane of the solar disc will lie anywhere along arc length LM which for small angles may be approximated by $\epsilon = \pm 3.5$ arc sec. If in addition, the ± 2.5 arc sec uncertainty of pitch and yaw is included, the actual commanded reference point will lie anywhere within region ABCD, which is the command point uncertainty (Figure 2). Since all angles are small, area ABCD may be considered to be a rectangle with a width of 5 arc sec (illustrated by ϵ_p) and a length of 12 arc sec (illustrated by ϵ_y) at an offset angle $\phi_o = 20$ arc min.

The control system stability requirements around any actual reference point are illustrated in Figure 3, where point A is considered as the actual commanded reference point. Arc length, PQ, in the plane of the solar disc is generated by the ± 7.5 arc min roll excursion during a 15-min time interval with a 20 arc min offset from the center of the sun. It may be approximated by an angle, ϕ_y, of ± 2.5 arc sec. The inclusion of pitch and yaw uncertainty of ± 2.5 arc sec generates the area EFGH, which is the locus of points for the control of the experiment package reference axis around the commanded reference point A. Since all angles are small, area EFGH may be approximated as a rectangle with a width of 5 arc sec (ϕ_p) and a length of 10 arc sec (ϕ_y), again assuming a 20 arc min offset angle. Since the center of area EFGH can be any point within area ABCD, the command pointing uncertainty may be combined with that for the control around an actual reference point. This results in an overall experiment package pointing uncertainty which may be approximated by a rectangle with a width of 10 arc sec and a length of 22 arc sec as illustrated in Figure 3.

CMG CONTROL SUBSYSTEM

The CMG control subsystem is a momentum exchange control system. The momentum exchange devices are three orthogonally-mounted double-gimbaled CMG's (Figure 4); each has a stored momentum capability of 2700 Nms. ATM cluster (Figure 1) moments of inertia and mass data are presented in Table III.
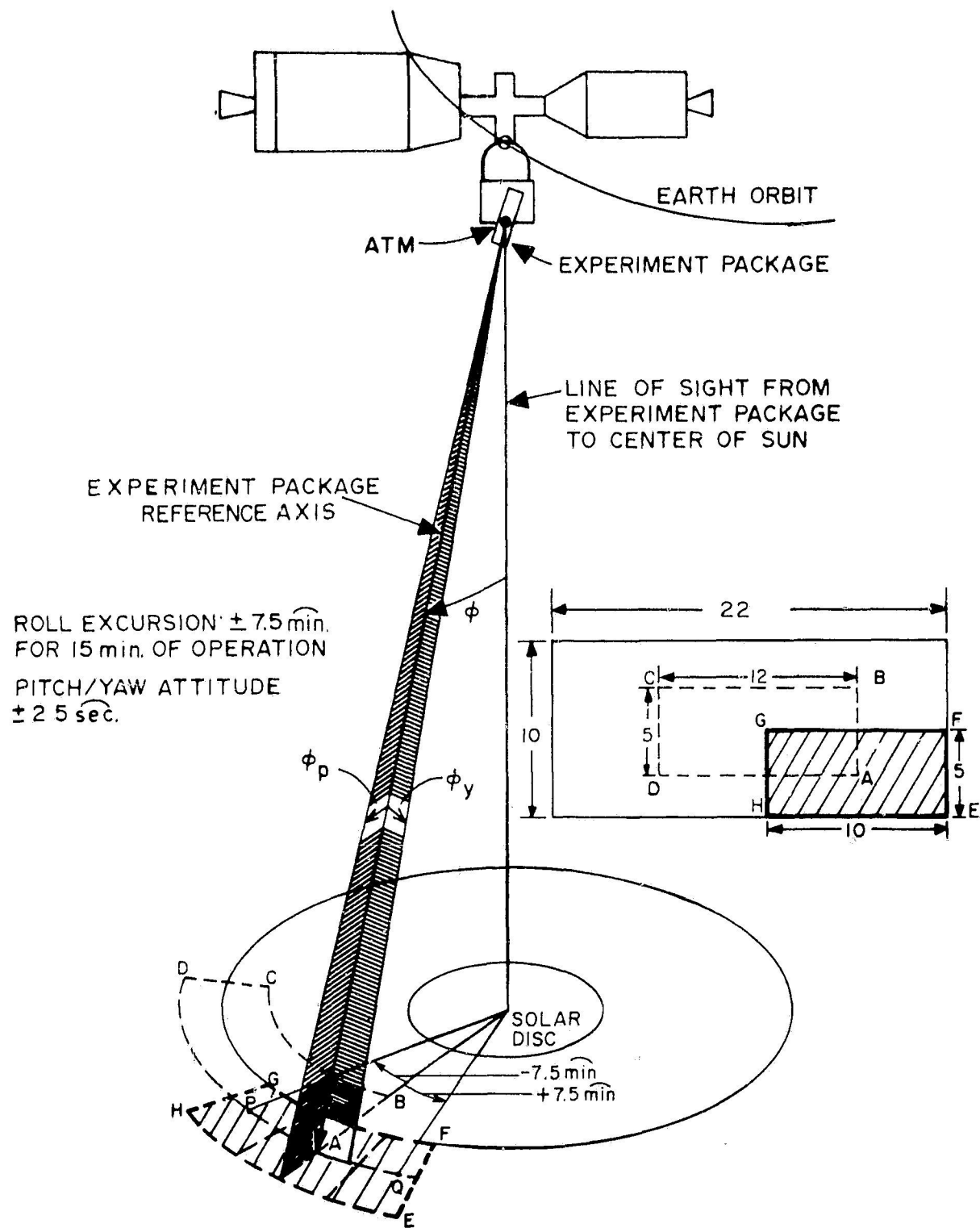
4

EARTH ORBIT

ATM

EXPERIMENT PACKAGE

EXPERIMENT PACKAGE
REFERENCE AXIS

LINE OF SIGHT FROM
EXPERIMENT PACKAGE
TO CENTER OF SUN

ROLL COMMAND POINTING
TOLERANCE $\phi_r = \pm 10\ \widehat{min}$

MAXIMUM OFFSET
RADIUS $\phi_o = 20\ \widehat{min}$

PITCH/YAW COMMAND POINT-
ING TOLERANCE: $\phi_{p,y} = \pm 2.5\ \widehat{sec}$

ϕ_o

ϵ

ϵ_p

ϵ_y

ACTUAL REFERENCE POINT
LIES IN AREA ABCD
WHICH IS COMMAND
POINT UNCERTAINTY

COMMANDED
POINT

C

B

D

A

5 sec

12 sec

D

C

B

A

M

ϕ_r

SOLAR
DISC

COMMANDED
POINT

$\sin \dfrac{\epsilon}{2} = \sin \phi_o \sin \dfrac{\phi_r}{2}$

$\epsilon \approx \phi_o\ \phi_r$ FOR SMALL ANGLES

$\therefore \epsilon \approx \pm 3.5\ \widehat{sec}$ FOR $\phi_o = 20\ \widehat{min}$. $\phi_r = \pm 10\ \widehat{min}$

FIGURE 2. COMMAND POINTING REQUIREMENTS

5

FIGURE 3. CONTROL REQUIREMENTS AROUND ACTUAL REFERENCE POINT (15-MIN PERIOD)

6
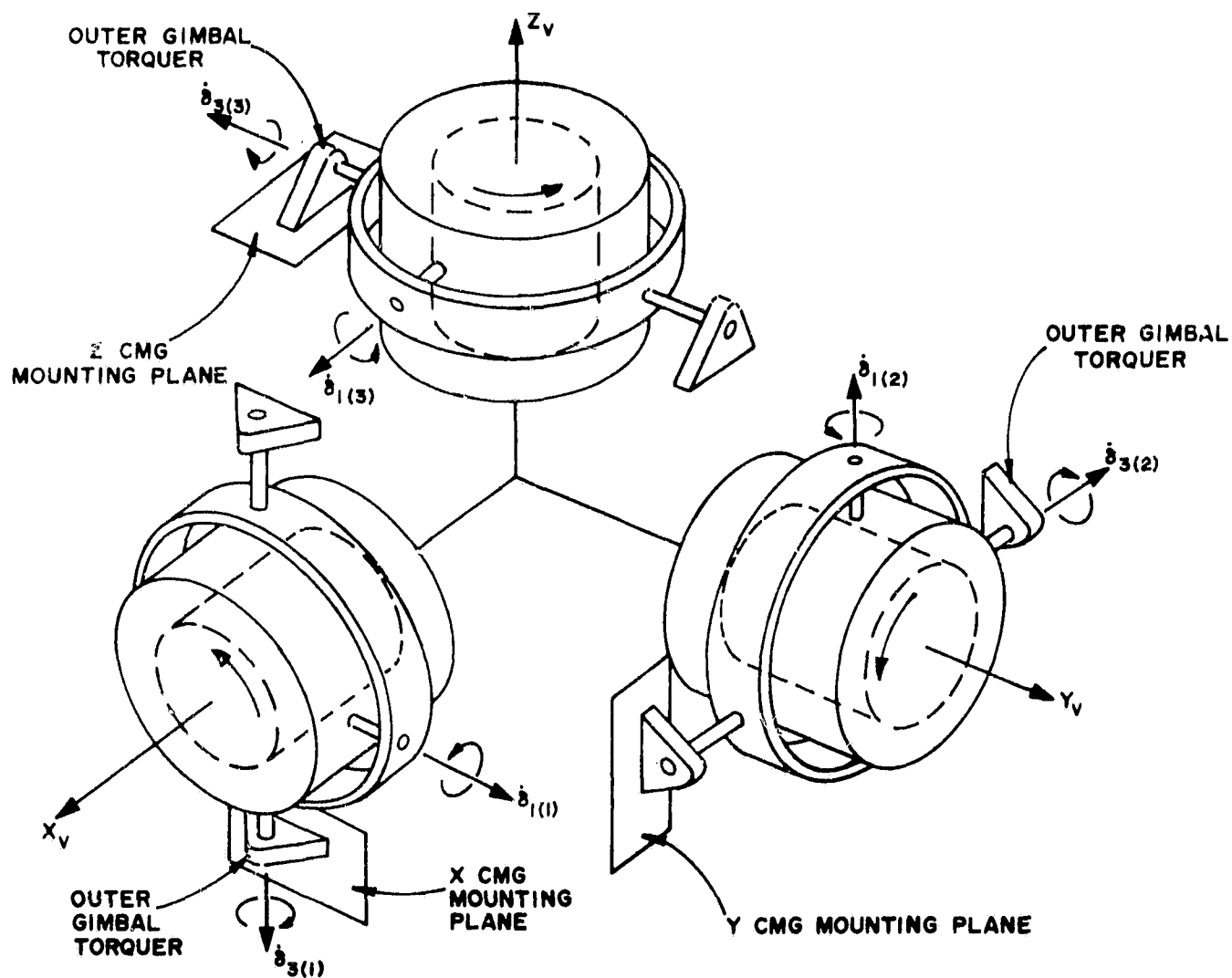
FIGURE 4. CMG CLUSTER

TABLE III. MOMENTS OF INERTIA
AND MASS OF ATM CLUSTER

I_1	=	0.8711 ×	10^6 kg·m^2
I_2	=	0.5497 ×	10^7 kg·m^2
I_3	=	0.5254 ×	10^7 kg·m^2
Mass	=	0.5409 ×	10^5 kg

The use of CMG's in the pointing and control of a large manned space station is new, and the problems associated with that type of system are unique and were unsolved. Some of the problems encountered in the development of the CMG control subsystem include the following:

1. An acceptable control law for use of the CMG's in control of the ATM cluster.

2. A means for preventing the CMG's from "falling into" an undesirable orientation such as that which would not allow the use of the CMG's to control

the spacecraft even though the CMG cluster was not in its saturated momentum state.

3. A means of desaturating the CMG cluster periodically without the use of a mass expulsion reaction control system (RCS). A method was needed to permit torques produced by an external force field such as gravity gradient to be used to effect CMG momentum desaturation.

4. The optimal orientation of the vehicle to minimize external bias torques which would tend to saturate the CMG cluster; i.e., the placement of the minimum principal axis of inertia into the orbital plane.

Acceptable control laws for use of the CMG's in control of the ATM cluster were ieveloped. A detailed derivation of these laws is given in References 1, 2, and 3. The basic concepts considered in the development of these control laws will be considered here. Figure 5 shows a schematic of a single CMG.
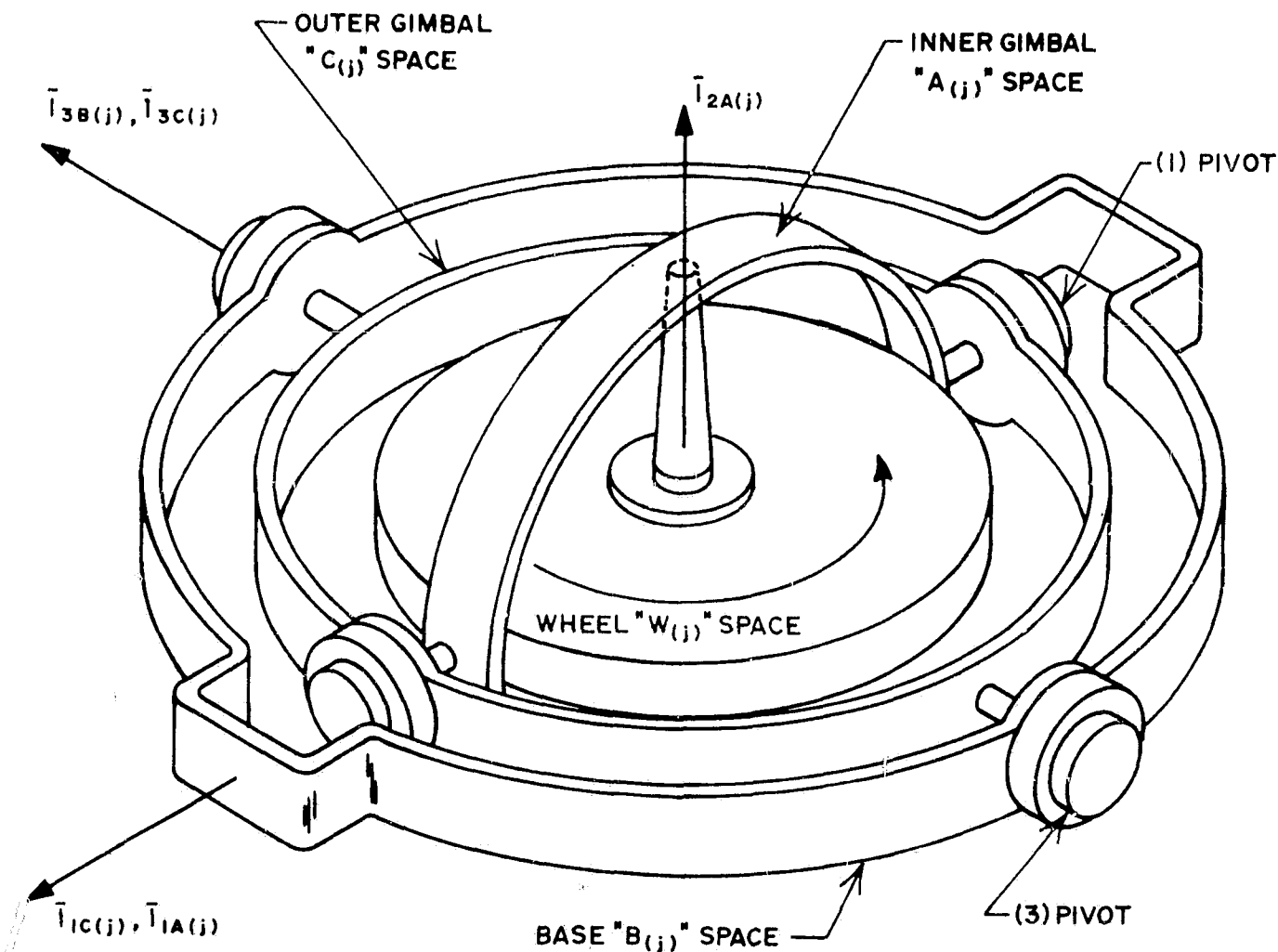

FIGURE 5. SCHEMATIC OF THE "j" CONTROL MOMENT GYRO

The CMG is a two-degree-of-freedom gyroscopic device used to generate controlled moments on its mounting base. It consists of a constant speed wheel held in a housing which is called the inner gimbal. The inner gimbal is coupled to the outer gimbal through a pivot which is perpendicular to the wheel spin vector. The outer gimbal is coupled to the base by the outer pivot. The two pivots are driven by geared torquers.

The reaction moment of an ideal cluster of CMG's on the vehicle can be expressed by equation (1).

$$\overline{M}_{RV} = - \left. \frac{d\overline{H}_{TI}}{dt} \right|_{\text{I-space}} = - \left[\left. \frac{d\overline{H}_{TV}}{dt} \right|_{V} + \overline{\omega}_{IV} \times \overline{H}_{TV} \right] \qquad (1)$$

where $\overline{H}_{TV}$ is the total angular momentum of the CMG cluster as expressed in vehicle space and $\overline{\omega}_{IV}$ is the inertial angular velocity of the vehicle.

Equation (1) can be simplified by expressing the individual momentum of each CMG in inner gimbal space as shown in equation (2).

$$M_{RV} = - \left(\left. \sum_{j=1}^{3} \frac{d\overline{H}_{A(j)}}{dt} \right|_{\text{A-space}} + \overline{\omega}_{VA(j)} \times \overline{H}_{A(j)} + \overline{\omega}_{IV} \times \overline{H}_{TV} \right) \cdot$$

$$(2)$$

With the assumption that $\overline{\omega}_{IV} \ll \overline{\omega}_{VA(j)}$ and a constant wheel speed;

i.e., $\left. \dfrac{d\overline{H}_{A(j)}}{dt} \right|_{\text{A-space}} = 0$, equation (2) reduces to equation (3).

$$\overline{M}_{RV} = - \sum_{j=1}^{3} \overline{\omega}_{VA(j)} \times \overline{H}_{A(j)} \qquad \cdot \qquad (3)$$

Equation (3) may be expressed in matrix form [1] relating the reaction moment about the various vehicle axes to the torquer rate commands on the individual CMG inner and outer gimbals, equation (4).

$$
\begin{bmatrix} M_{RXV} \\ M_{RYV} \\ M_{RZV} \end{bmatrix} = [A] \begin{bmatrix} \dot{\delta}_{1(1)} \\ \dot{\delta}_{1(2)} \\ \dot{\delta}_{1(3)} \\ \dot{\delta}_{3(1)} \\ \dot{\delta}_{3(2)} \\ \dot{\delta}_{3(3)} \end{bmatrix} \tag{4}
$$

The six CMG relative gimbal rates must be commanded, based upon information derived from body-mounted attitude and rate sensors. Since these sensors are aligned to the geometric body axes, they provide information relative to these three axes only. This three-dimensional information must now be routed or "steered" to provide six commanded CMG gimbal rates which would produce a reaction moment to optimally cancel any disturbance moment. The law that governs this generation of a six-dimensional vector, based upon three-axis information, is called the steering law, which is given in generalized form by equation (5).

$$
\begin{bmatrix} \dot{\delta}_{1(1)C'} \\ \dot{\delta}_{1(2)C'} \\ \dot{\delta}_{1(3)C'} \\ \dot{\delta}_{3(1)C'} \\ \dot{\delta}_{3(2)C'} \\ \dot{\delta}_{3(3)C'} \end{bmatrix} = [T_s] \begin{bmatrix} M_{CXV} \\ M_{CYV} \\ M_{CZV} \end{bmatrix} \tag{5}
$$

where M_{CXV} is the commanded moment about the $\bar{1}_{XV}$ vector based on body-mounted sensor information. $[T_s]$ is the steering law. $\dot{\delta}_{i(j)c'}$ is the commanded gimbal rate of the ith pivot of the jth CMG.

Assuming that $\dot{\delta}_{i(j)c} = \dot{\delta}_{i(j)}$ and combining equations (4) and (5), we arrive at an expression that relates the commanded to the actual vehicle torques as shown in equation (6).

$$\begin{bmatrix} M_{RXV} \\ M_{RYV} \\ M_{RZV} \end{bmatrix} = [A][T_s] \begin{bmatrix} M_{CXV} \\ M_{CYV} \\ M_{CZV} \end{bmatrix} \tag{6}$$

To optimally control the CMG cluster, we require the matrix $[A][T_s]$ to be an identity $[A][T_s] = [I]$; this requires the steering law matrix to be the inverse of the CMG cluster matrix $[A]$. However, since $[A]$ is not a square matrix, no inverse exists and any attempt to get an inverse results in a steering law which exhibits no control for many CMG gimbal angle combinations. This approach at formulating a steering law fails and another approach must be sought.

A close inspection of equation (3) reveals that to nullify a disturbance torque, the H-vector of each CMG must be made to swing into the direction of the disturbance torque. Based on this consideration, a steering law (the cross product steering law) can be postulated by equation (7).

$$\bar{\omega}_{VA(j)C'} = K_{SL} \bar{1}_{2A(j)} \times \bar{\alpha}_{TV} \tag{7}$$

where $\bar{\omega}_{VA(j)C'}$ is the commanded j^{th} CMG momentum vector rate relative to vehicle space. K_{SL} is a constant. $\bar{1}_{2A(j)}$ is the unit vector along the spin vector of the jth CMG. $\bar{\alpha}_{TV}$ is a vector based on vehicle body sensor information and thus indicates the direction of the disturbance moment.

Carrying out the necessary equation development [1] yields the CMG cluster steering law and the desired relationship between the commanded gimbal rates and disturbance moment information.

$$
\begin{bmatrix}
\dot{\delta}_{1(1)C'} \\
\dot{\delta}_{1(2)C'} \\
\dot{\delta}_{1(3)C'} \\
\dot{\delta}_{3(1)C'} \\
\dot{\delta}_{3(2)C'} \\
\dot{\delta}_{3(3)C'}
\end{bmatrix}
= K_{SL}[T_s]
\begin{bmatrix}
\alpha_{TVXV} \\
\alpha_{TVYV} \\
\alpha_{TVZV}
\end{bmatrix}
\tag{8}
$$

The steering law previously developed would fall far short of the goal if used directly to control the CMG cluster; i.e., to have an invariant forward gain with a minimization of cross-coupling torques.

The "H-vector control law," developed in Reference 2, is a closed loop controller which, when used with the cross-product steering law, provides an almost optimal CMG cluster control law.

The H-vector control law scales the $\overline{\alpha}_{TV}$ vector to be a commanded torque. The commanded torque vector is then electronically integrated and compared to the angular momentum of the CMG cluster. The error momentum vector is then nulled by driving the six CMG gimbals with the aid of the steering law.

A simplified diagram of the H-vector control law is shown in Figure 6.

Because of the nonuniqueness of the H-vector control law and its associated cross-product steering law, the requisite CMG gimbal angles to produce a given total momentum vector are not uniquely defined. If the required total momentum vector is 1H , then the CMG cluster can attain an undesirable orientation in which all three CMG spin vectors are colinear. This orientation
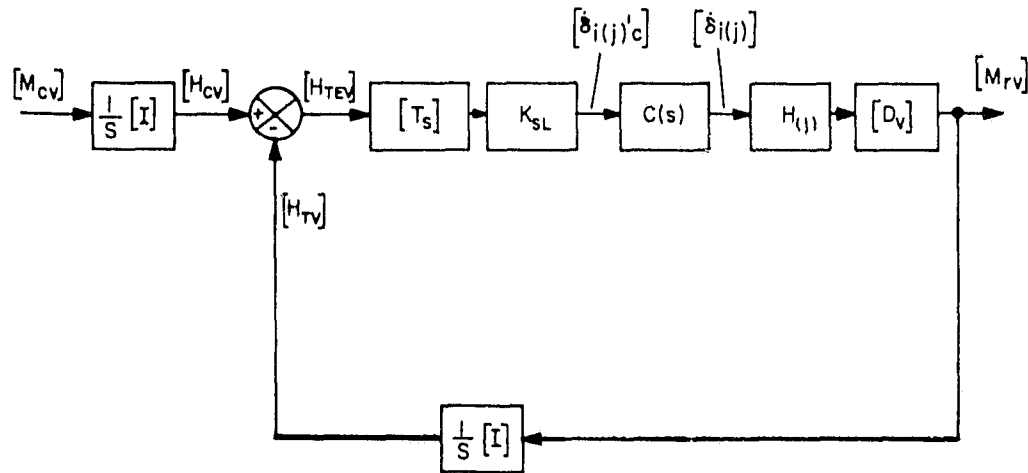
FIGURE 6. H-VECTOR CONTROL LAW

has been called the "anti-parallel" case. The CMG cluster, when in the anti-parallel orientation, exhibits zero gain along the axis of colinearity. Thus, if a disturbance torque were applied along this axis, the CMG's would not be able to compensate for it even though they are not saturated. This problem prompted an investigation that resulted in the development of the "isogonal distribution and rotation laws." A brief description of these laws is now presented. Reference 3 treats this subject in detail.

For any given total angular momentum vector, it is desirable to place the three individual spin vectors into an orientation in which each contributes an equal component along the total vector. This constraint results in equal angles between the individual vectors and the total. This distribution is called an isogonal distribution and utilizes two of the remaining three degrees of freedom of the CMG cluster (the H-vector control law utilizes three degrees of freedom). It can be shown that the remaining degree of freedom is only a rotation of the three individual momentum vectors about the total vector. This last degree of freedom is used to minimize the inner gimbal angles of the CMG's.

The isogonal distribution and rotation laws generate six commanded bias rates for the six CMG gimbals. These bias rates are added to the commanded rates as derived from the cross-product steering law.

Essentially, the bias rates can be considered as the sum of the two rates; one from the distribution law $\dot{\delta}_{Di(j)}$ and the other from the rotation law $\dot{\delta}_{Ri(j)}$,

$$\dot{\delta}_{i(j)BC} = \dot{\delta}_{Di(j)} + \dot{\delta}_{Ri(j)} \quad . \tag{9}$$

13

In addition to eliminating the possibility of "falling into" the anti-parallel case, the isogonal distribution and rotation law has also improved the performance of the CMG cluster by extending the bandwidth of the direct gain and by reducing the cross-coupling torques. This improvement is shown by inspecting Figures 7 and 8 which show the direct and cross-coupling frequency response of the CMG cluster with and without the distribution and rotation laws (for the same total momentum).
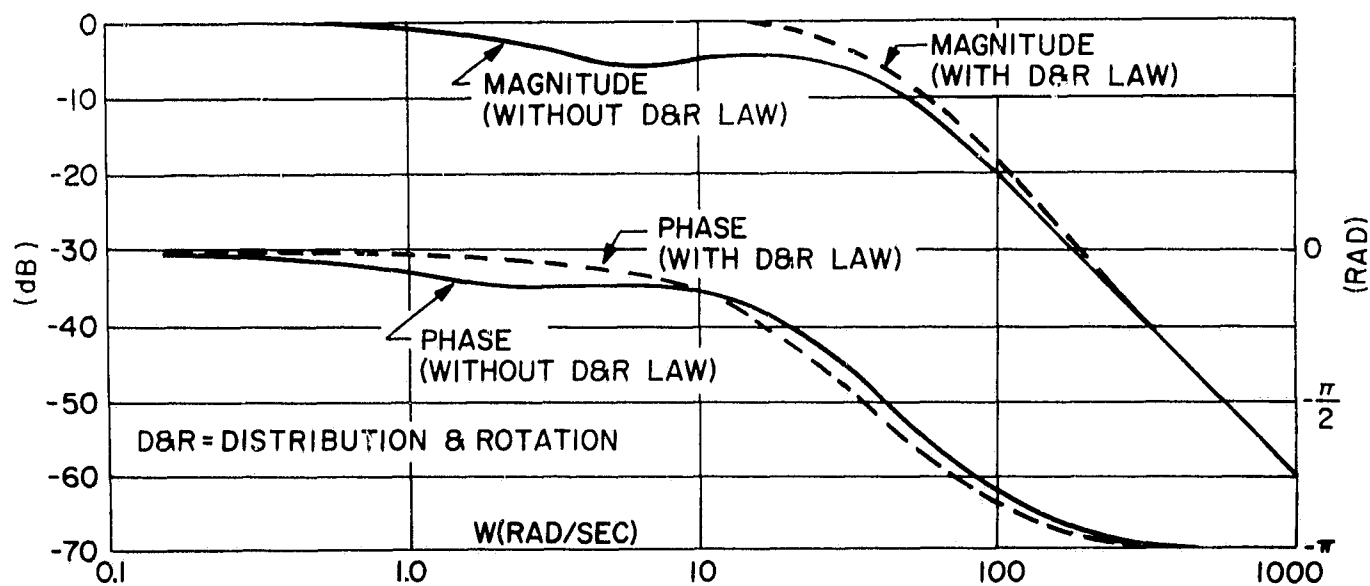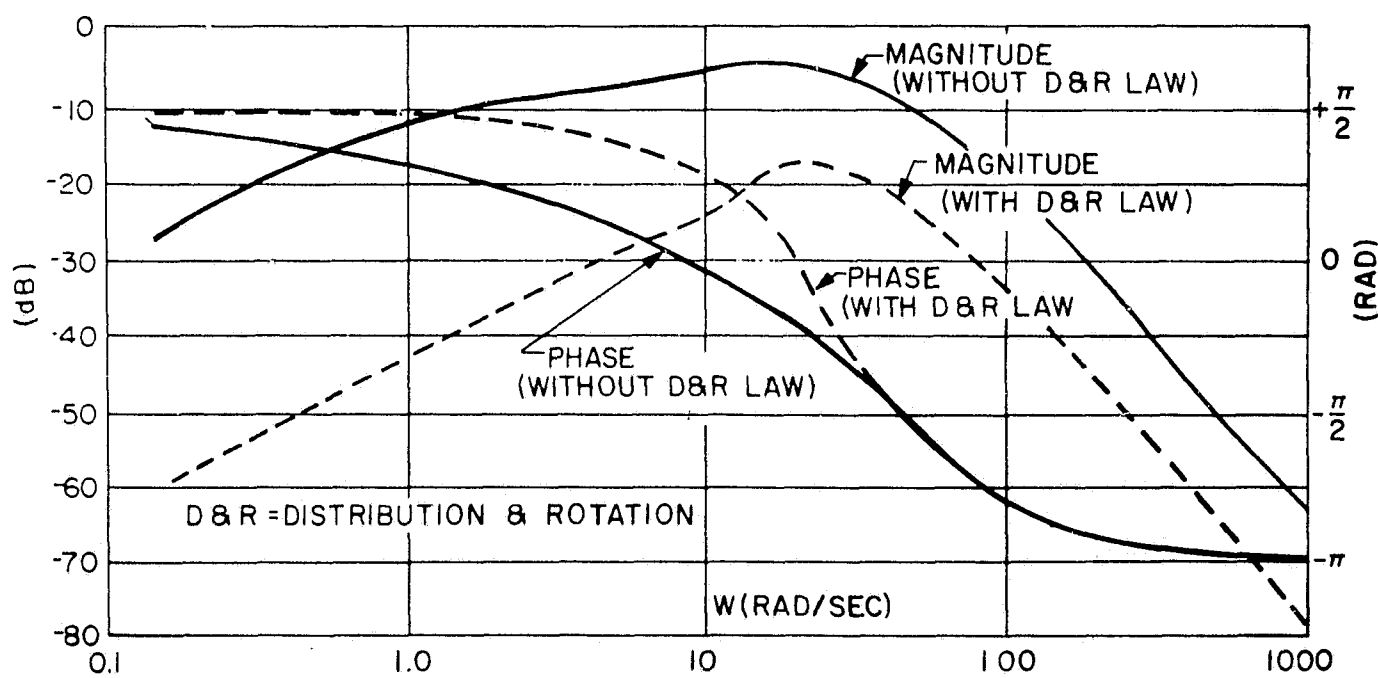

FIGURE 7. H-VECTOR CONTROL LAW RESPONSE Mrx/Mcx

FIGURE 8. H-VECTOR CONTROL LAW RESPONSE Mrx/Mcz

14

Figure 9 shows an anti-parallel configuration and a possible orientation with the aid of the distribution and rotation laws.

ANTI-PARALLEL CONDITION   WITH DISTRIBUTION & ROTATION LAWS
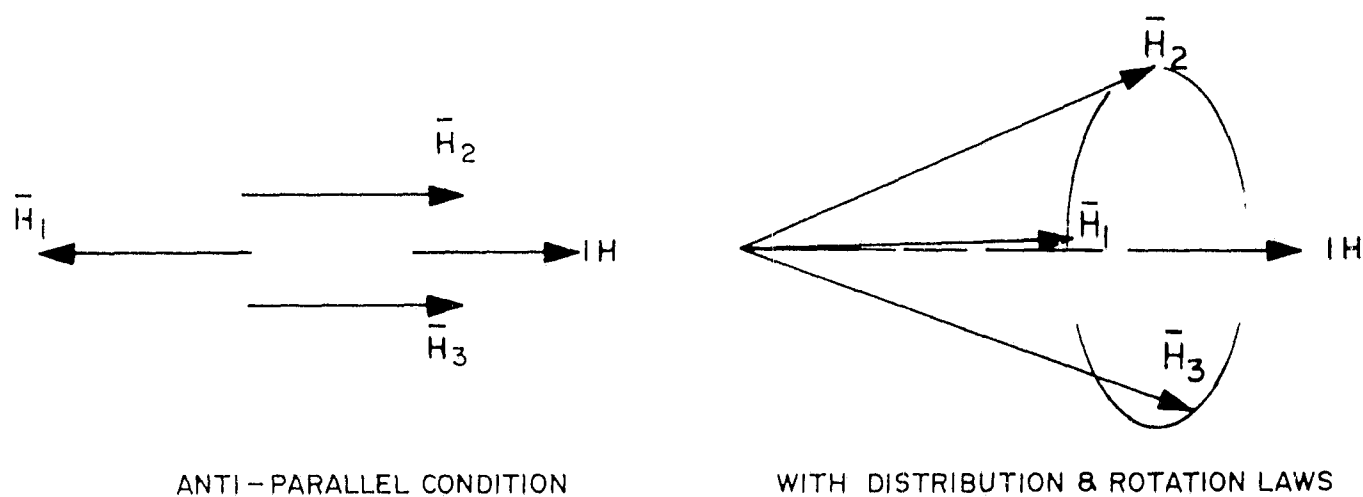
FIGURE 9. H-VECTOR CONFIGURATION

The developed CMG control system including its numerous nonlinearities was simulated on a large hybrid computer. The system operated in a satisfactory manner for small initial conditions (0.1 to 0.5 degree) and slowly varying external torques (gravity gradient, etc.). If, however, the initial CMG orientation was highly nonisogonal or if two-CMG operation was considered, it was found that oscillatory and, in some cases, unstable operation resulted.

This was remedied by adding a variable gain feedback term from the "H" error signal to the input of the H integrator. A simplified diagram of the system, as now designed, is shown in Figure 10.

To desaturate the CMG cluster, periodically, without the use of a mass expulsion reaction control system, a method was developed utilizing the earth's gravity-gradient force field to effect CMG momentum desaturation. The method developed is described in detail in Reference 4. The basic concept is best described with the aid of Figure 11 which depicts the per orbit momentum build-up of the CMG cluster caused by gravity gradient and aerodynamic torques. A careful inspection of this figure reveals that if periodic CMG desaturation were not provided, the CMG cluster would be saturated for progressively larger portions of an orbit after the first orbit. The axis of saturation would be roughly the vehicle X axis. This means that after complete saturation, the CMG cluster could not compensate for a disturbance torque about the axis of saturation.
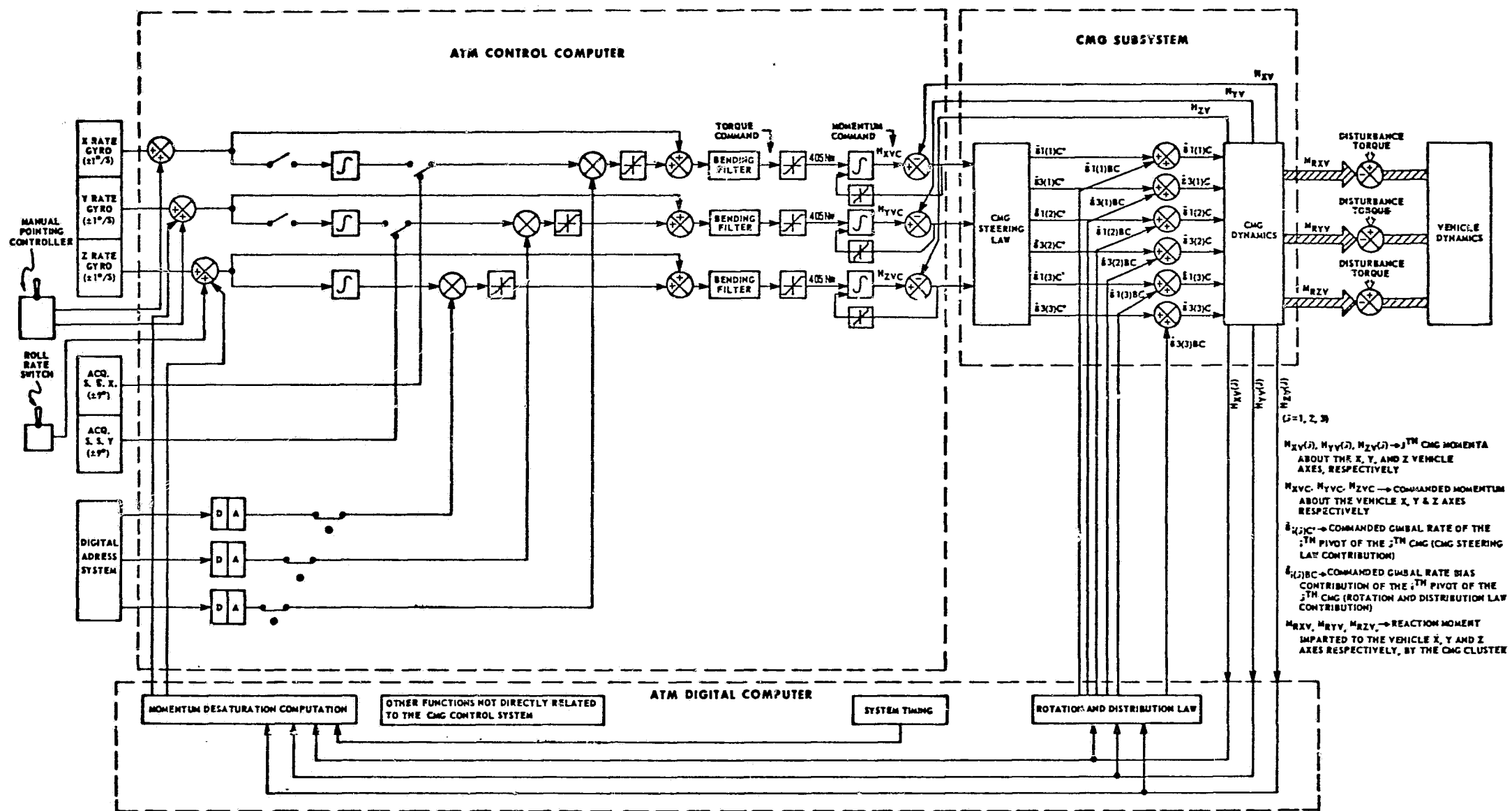
15

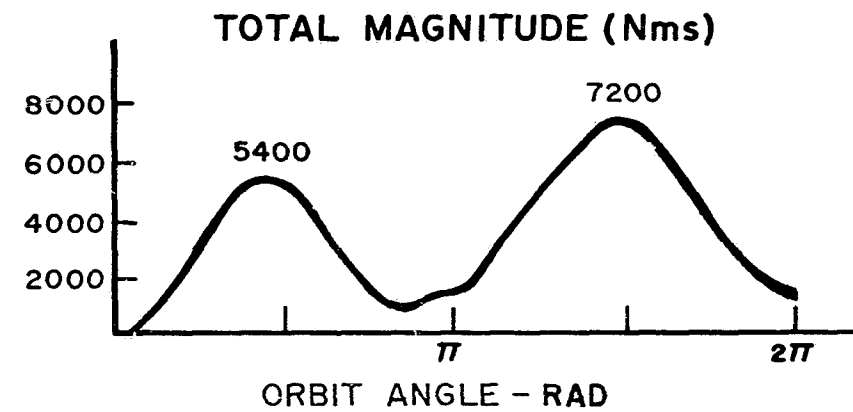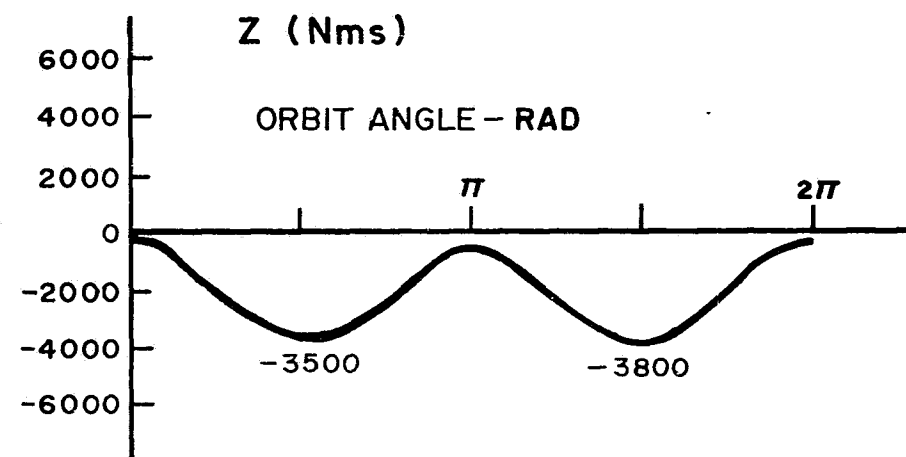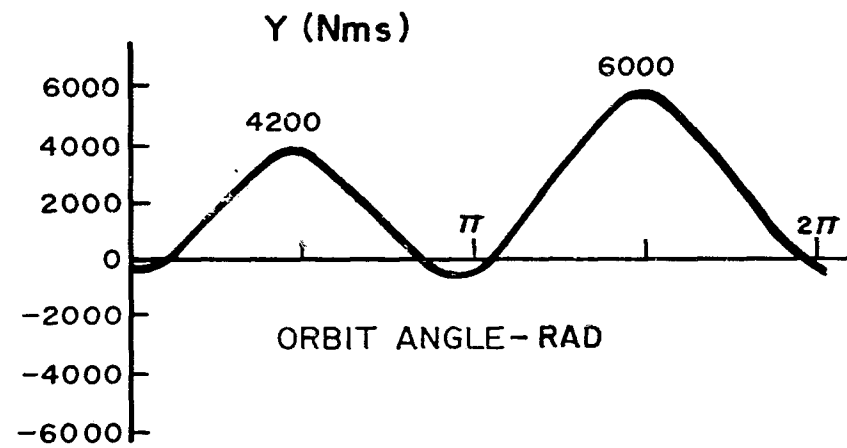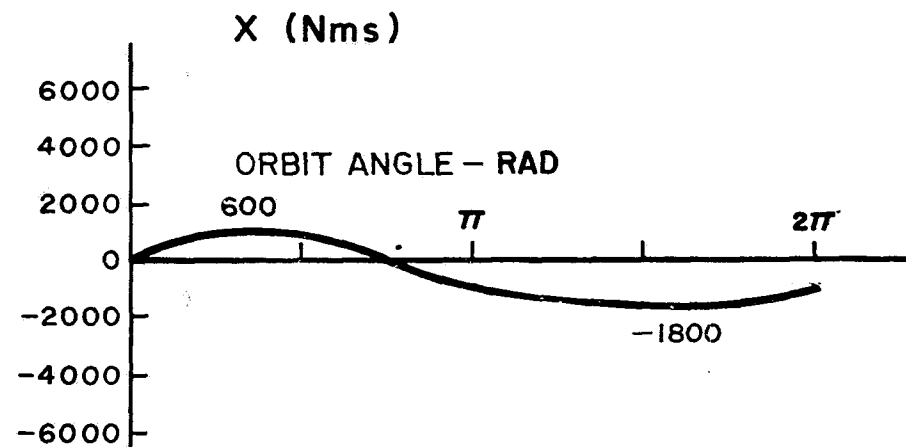FIGURE 10. ATM FUNCTIONAL BLOCK DIAGRAM POINTING CONTROL SUBSYSTEM (CMG CONTROL)

FIGURE 11. COMBINED DISTURBANCE IMPULSE (SOLAR INCLINATION = - 30 DEGREES)

An investigation of the causes of the predominant noncyclic torques (i.e., gravity gradient and aerodynamic) reveals that with the given vehicle configuration and mission requirements (i.e., point vehicle Z axis at radiometric center of sun every daylight period), it is not possible to eliminate the noncyclic torques but it is possible to minimize them.

This problem of CMG momentum management was attacked in two separate ways.

1. The noncyclic disturbance torques were minimized by finding an optimal vehicle orientation while still meeting the requirement that vehicle Z axis point to the center of the solar disk. This was accomplished by sampling the vehicle momentum at a specified time during the daylight orbital period and comparing it with the previous day's sample. The compared sample indicated whether the bias momentum components about the various vehicle axes were increasing or decreasing. This information was then translated into appropriate angle position commands about the vehicle Z axis to ensure minimization of bias momentum accumulation.

2. The saturation effects of the remaining noncyclic disturbance torques were nullified by periodically producing controlled bias torques which would tend to desaturate the CMG cluster. The controlled bias torques are produced by employing rectified components of the gravity gradient torques encountered during the night portion of the orbit to desaturate the CMG cluster. The rectification of the gravity gradient torques is made possible by maneuvering the vehicle about two axes during the night side of the orbit. The magnitude of the maneuver angles is a function of the momentum accumulation during the daylight portion of the orbit.

EPC CONTROL SUBSYSTEM

The EPC control system utilizes flex-pivot gimbal bearings for control about two axes and an open-loop positioning device to meet positioning requirements about the third axis. The flex pivots allow approximately ±2 degrees of rotation of the X and Y axes while the roll positioning device allows for a rotation of ±120 degrees about the experiment package Z axis. A block diagram of this system is shown in Figure 12.

While the EPC provides automatic control of the experiment package X and Y axes, manual positioning of these two axes is provided for the purpose

RATE GYRO

$$\frac{K_{RG}}{S^2 + 2\zeta\omega_N S + \omega_N^2}$$

AMP. # 1

$$\frac{K_a}{\tau_a S + 1}$$

TORQUER # 1

K_m

T_c

FINE SUN SENSOR

$$\frac{K_{FS}}{S\tau_{FS} + 1}$$

AMP. # 2

$$\frac{K_a}{\tau_a S + 1}$$

TORQUER # 2

K_m

T_D

T_c

SOLAR VECTOR

OPTICAL WEDGE DRIVE

HAND CONTROLLER

PITCH COMMAND
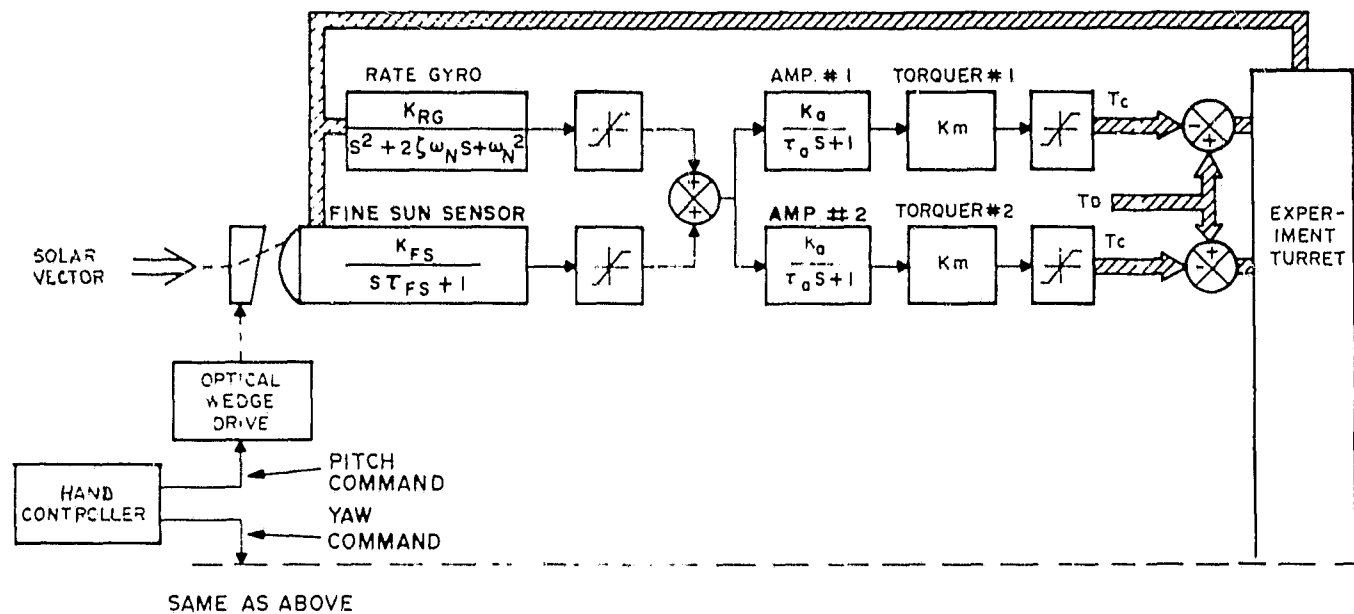
YAW COMMAND

EXPERIMENT TURRET

SAME AS ABOVE

FIGURE 12. EXPERIMENT POINTING AND CONTROL SUBSYSTEM

of offset pointing. Fine sun sensors (FSS) are used for sensing spar attitude errors, with rate gyros sensing rates. The ATM control computer (ATMCC) conditions the sensors' signals to provide rate plus displacement command signals to the flex-pivot actuators (dc torque motors).

The experiment package can be offset pointed in the X and Y axes over a range of ±20 arc min, with the center of the solar disk being the zero position. The solar disk measures approximately 32 arc min from limb to limb. Offset pointing is accomplished by positioning an optical wedge located in each of the FSS. The wedge is mounted in the path of the sunlight passing through the FSS optics and can be rotated to refract the sunlight a fixed angle in a controlled direction. The wedges are positioned by a drive mechanism controlled by the astronaut via the manual pointing controller. The wedge drive varies from ±135 arc sec/sec near zero offset positions to 76 arc sec/sec for wedge positions near the 20 arc min sun offset position. A wedge offset produces an FSS output error voltage that causes the spar to rotate about the appropriate axis (X or Y) and point the FSS, and thereby the experiment package, in a direction that will drive the FSS output voltage to null. Stability is then automatically maintained by the EPC. The experiments are aligned to the FSS. The position of each FSS wedge is displayed on the PCS control and display panel and corresponds to the experiment package offset position from the center of the sun in the X or Y axis. The panel also contains television displays of the sun, as viewed through experiment telescopes, and experiment readout displays to assist the astronaut in pointing the experiment package.

19

The roll positioning mechanism (RPM) is used to rotate the spar about the Z axis. The mechanism is commanded by the astronaut via the manual pointing controller (rate switches) located on the control and display panel. Spar roll rates of ±7, ±3.5, ±0.7, and ±0.35 degrees per second can be commanded. Once the spar is positioned, the RPM will hold the location until a repositioning command is received. The astronaut repositions the spar in accordance with experiment demand requirements. The spar roll position is displayed on the control and display panel.

ATM POINTING CAPABILITY

The ATM pointing and stability requirements listed in Table II were developed as a result of the various individual ATM experiment pointing and stability requirements. The ability of the ATM pointing and control system to meet these requirements was established analytically by performing a detailed error analysis of the system. This analysis is being continually updated as additional input data become available. A Monte Carlo procedure was employed for the determination of system position and rate output errors for various model configurations of both the CMG control system and the EPC system [5]. System dynamics were evaluated on hybrid computer simulations of the system [6]. The results of these studies are summarized in Tables IV and V. The numbers not in parentheses are system requirements while those within the parentheses represent the presently estimated 2σ system capability.

TABLE IV. EPC CONTROL SYSTEM POINTING CAPABILITY 2σ

System Axis	Pointing Uncertainty	Stability for 15 Min
EPC X	±2.5 arc sec (1.77 arc sec)	±2.5 arc sec (0.63 arc sec)
EPC Y	±2.5 arc sec (1.77 arc sec)	±2.5 arc sec (0.63 arc sec)
EPC Z Roll reference	±10 arc min (±7.0 arc min)	CMG control system

TABLE V. CMG CONTROL SYSTEM POINTING CAPABILITY 2σ

System Axis	Pointing Uncertainty	Stability for 15 Min
CMG X	±4 arc min (±2.75 arc min)	±9 arc min (±3.6 arc min)
CMG Y	±4 arc min (±2.75 arc min)	±9 arc min (±5.7 arc min)
CMG Z	±10 arc min (±0.624 arc min)	±7.5 arc min (±5.0 arc min)

The main errors associated with the EPC systems' pitch and yaw control were those caused by FSS null accuracy (±1.4 arc sec) and FSS wedge readout resolution (±1.25 arc sec). The effect of man-motion disturbances was nearly negligible; the most significant being ±0.2 arc sec position displacement as a result of astronaut wall pushoff disturbance (Figure 13). The main error source in experiment roll reference determination is due to RPM readout and positioning errors which are on the order of ±5 arc min (2σ).

The error sources associated with the CMG control system pointing uncertainty are due mainly to an accumulation of various electronic gain null offset and drift terms. The stability error source is the result of astronaut wall pushoff disturbances.

CONCLUSIONS

Based upon high accuracy pointing requirements, an ATM pointing and control system has been developed to meet experiment objectives. A significant portion of the PCS is capable of manual operation. Astronaut operation is thus available to perform various functions such as those which require judgment to select scientific targets and to point experiments to these targets. To keep the number of tasks required by the astronaut within reason, many functions such as attitude pointing stability are performed using closed-loop automatic control. However, because of the manual control capability and television optics display system, the astronaut can manually improve some of these functions such as offset pointing and experiment line-of-sight calibration.
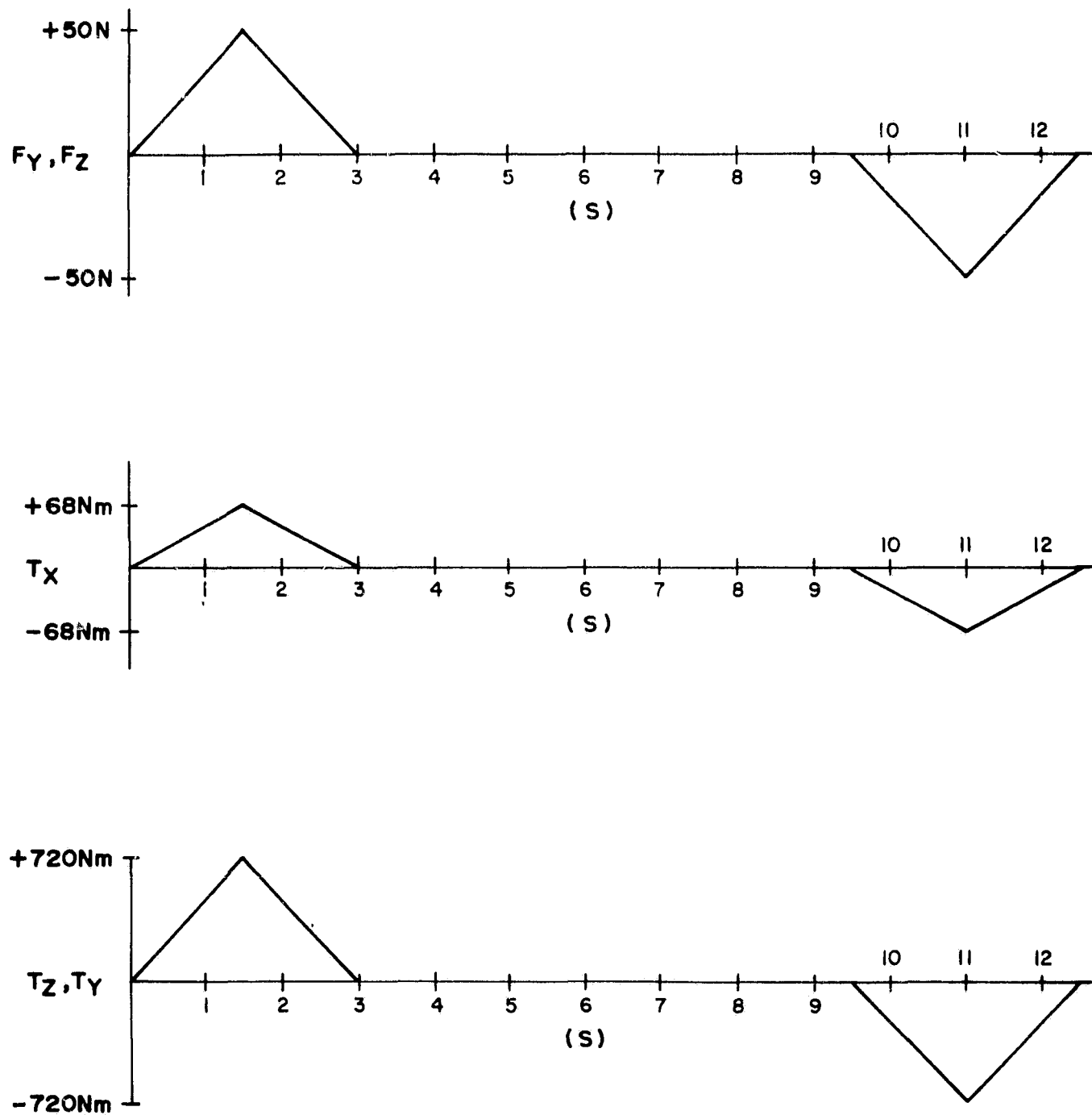
FIGURE 13. ASTRONAUT WALL PUSHOFF DISTURBANCE

The system is unique in that it utilizes the energy source of its operating environment to effect the desired pointing and control requirements of the space station. The electrical energy required to power the experiments and the pointing and control system are supplied through onboard storage devices via large solar panels. The principal disturbance torques are cyclic, and the momentum storage and dissipation characteristics of the CMG's are ideally

suited to operation in this type of environment. The accumulation of momentum by those noncyclic torques is compensated for by maneuvering the space station during the night portion of the orbit against the gravity gradient field in such a manner as to nullify the noncyclic bias torque effect.

The developed pointing and control systems meet the experiment pointing requirements. The same type of system with improved electronics, sensors, and some minor limitations on astronaut motion during observation periods might achieve pointing accuracies on the order of 0.1 to 0.01 arc sec [7].

REFERENCES

1. Chubb, W. B., and Epstein, M.: Application of Control Moment Gyros in the Attitude Control of the Apollo Telescope Mount. AIAA Paper No. 68-866, August 1968.

2. Morine, L. A., and O'Connor, B. J.: A Description of the CMG and Its Application to Space Vehicle Control. AIAA Paper No. 67-589, August 1967.

3. Kennel, H. F.: Individual Angular Momentum Vector Distribution and Rotation Laws for Three Double-Gimbaled Control Moment Gyros. Marshall Space Flight Center, NASA TMX-53696, January 1968.

4. Kennel, H. F.: Angular Momentum Desaturation for ATM Cluster Configuration Using Gravity Gradient Torques. Marshall Space Flight Center, NASA TMX-53748, May 27, 1968.

5. Blue, J. C., and Margosian, Z.: AAP Payload Integration Technical Report, "PCS Static Error Budget Analysis Report." ED 20002-551, Martin Marietta Corporation, Denver Division, June 28, 1968.

6. Kimery, R.: Stability Analysis of Experiment Pointing Control System. S.P. 213-0160, Space Support Division, Sperry Rand Corporation, Huntsville, Alabama, December 17, 1968.

7. Smith, P. G.: Astronomy Manned Space Flight Attitude Control Telescope Systems. Technical Memorandum TM 69-1022-2, Bellcomm Inc., Washington, D.C., February 17, 1969.
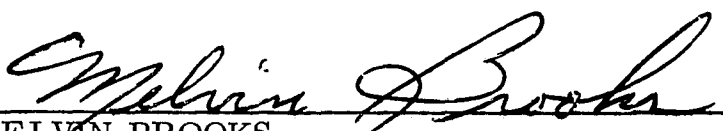
APPROVAL

STABILIZATION AND CONTROL OF THE APOLLO TELESCOPE MOUNT

By W. B. Chubb

The information in this report has been reviewed for security classification. Review of any information concerning Department of Defense or Atomic Energy Commission programs has been made by the MSFC Security Classification Officer. This report, in its entirety, has been determined to be unclassified.

This document has also been reviewed and approved for technical accuracy.

MELVIN BROOKS
Chief, Guidance and Control Systems Branch

F. S. WOJTALIK
Chief, Systems Division

F. B. MOORE
Director, Astrionics Laboratory